Applied Mathematical Sciences, Vol. 9, 2015, no. 65, 3227 - 3237
HIKARI Ltd, www.m-hikari.com
http://dx.doi.org/10.12988/ams.2015.54310

Couple Stress Fluids in Porous Circular Squeeze Films

P. Vimala

Department of Mathematics
Anna University Chennai – 600025, India

G. Sumathi

Department of Mathematics
Adhiparasakthi College of Engineering
Melmaruvathur – 603319, India

Abstract

The squeeze film flow characteristics of a couple stress fluid between porous circular disks is investigated. The modified Reynold's equation is derived using Stokes microcontinuum theory and is solved analytically. The expressions for the squeeze film pressure and the squeeze film force are obtained in terms of Fourier-Bessel series. Numerical results are presented for the sinusoidal motion of the upper porous disk. Further, the equation for the gap width between the disks is obtained by considering a constant force squeezing state and is solved numerically. The effects of couple stresses and the porous facing on the squeeze film behaviour are analysed through the squeeze film pressure, force and the film thickness as a function of response time.

Keywords: Porous Squeeze Films, Hydrodynamic Lubrication, Couple Stresses

1 Introduction

Squeeze film mechanism is commonly observed in many areas of engineering and applied sciences, such as bearings in automotive and aircraft engines, turbo machinery, squeeze film dampers, etc. A squeeze film is a thin layer of fluid situated between surfaces that are approaching each other. This approaching action of

the surfaces, forces the fluid layer to move towards less constrained surroundings. As the fluid layer is very thin, the viscous forces become dominant and offer high resistance to such fluid motion inhibiting the approach of the bounding surfaces which in turn reduces the wear and tear of the parts. Thus a squeeze film plays a major role in many lubrication problems. Many investigations discuss about the squeeze film characteristics of Newtonian or non-Newtonian fluids in non-porous geometries [5, 6, 11, 14, 15].

Porous bearings have been widely used in industry for a long period of time. Porous bearings contain the porous medium filled with lubricating oil so that the bearings require no further lubrication during the whole life of the machine. Self-lubricated bearings or oil retaining bearings exhibit this feature. There have been numerous studies on various types of porous bearings considering the lubricant as a Newtonian fluid. The squeeze film behavior of a Newtonian fluid has been analyzed between porous rectangular plates [17], porous journal bearings [4] and porous circular disks [7].

Owing to the development of modern machinery, the use of fluids blended with various kinds of additives has received a great attention in literature. Many micro-continuum theories [1, 2] have been developed to explain the peculiar behavior of these kinds of non-Newtonian fluids. Among all, Stokes theory [13] is considered as the simplest generalization of the classical continuum theory which accounts for the polar effects such as couple stresses, body couples and non-symmetric stress tensors. Many investigators have applied this couple stress fluid model to study the hydrodynamic bearing characteristics [12, 16]. These investigations have shown the significance of couple stress effects on the squeeze film behavior in non-porous geometries.

Several investigations reveal the combined effects of couple stresses and surface roughness between various geometries with one porous facing [3, 8, 9]. Naduvinamani et al. [10] have examined the rheological effects of the couple stress fluids on the squeeze film behavior in porous journal bearings.

In this paper, the flow of couple stress fluid between porous circular disks is considered. On the basis of Stokes micro-continuum theory, the modified Reynold's equation is derived and is solved analytically. The equation for the gap width is obtained by considering a constant force squeezing state. The results are obtained assuming a sinusoidal motion of the upper disk. The effects of couple stresses and porosity are investigated through the squeeze film pressure, squeeze film force and the film thickness as a function of response time.

2 Mathematical Formulation

Figure 1 shows the squeeze film geometry between circular disks of radius r_a lubricated with an incompressible couple stress fluid. The upper disk with porous facing at $z = h(t)$ is approaching the lower impermeable disk at $z = 0$ with a normal velocity dh/dt.

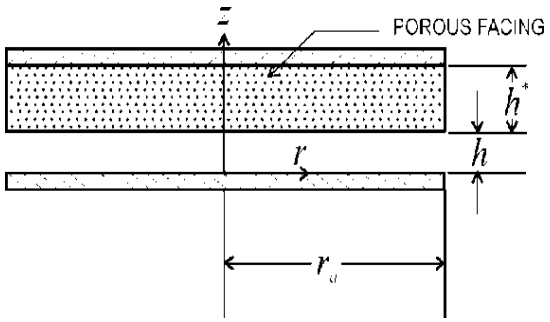

Figure 1 Squeeze Film in Porous Circular Geometry

Using the hydrodynamic lubrication theory, the flow is assumed to be axisymmetric and laminar and the body forces are assumed to be absent. According to Stokes microcontinuum theory, the body couples are also assumed to be absent. Under these assumptions, the governing equations of motion of the incompressible couple stress fluid flow are

$$\frac{1}{r}\frac{\partial(ru)}{\partial r}+\frac{\partial w}{\partial z}=0 \tag{2.1}$$

$$\frac{\partial p}{\partial r}=\mu\frac{\partial^2 u}{\partial z^2}-\eta\frac{\partial^4 u}{\partial z^4} \tag{2.2}$$

$$\frac{\partial p}{\partial z}=0 \tag{2.3}$$

where u and w are the velocity components in the radial and axial directions respectively, p is the squeeze film pressure, ρ is the fluid density, μ is the shear viscosity and η is the new material constant responsible for the couple stress property with the dimension of momentum.

The flow of couple stress fluid in the porous matrix is governed by the modified form of Darcy's law which accounts for polar effects given by

$$u^*=\frac{-\kappa}{\mu(1-\beta)}\frac{\partial p^*}{\partial r} \tag{2.4}$$

$$w^*=\frac{-\kappa}{\mu(1-\beta)}\frac{\partial p^*}{\partial z} \tag{2.5}$$

where u^* and w^* are respectively the radial and axial components of the fluid velocity in the porous region, p^* is the film pressure in the porous region, κ is the permeability of the porous facing and the parameter $\beta=(\eta/\mu)/\kappa$ is the ratio of microstructure size to the pore size. The ratio η/μ has a dimension of length square and this length may be regarded as the chain-length of the polar additives.

If $\eta/\mu \approx \kappa$, *i.e.* $\beta \approx 1$, then the microstructure additives present in the lubricant, block the pores in the porous layer and thus reduce the Darcy flow through the porous matrix. When the microstructure size is very small when compared to the pore size, *i.e.* $\beta \ll 1$, the additives percolate into the porous matrix which is the ideal situation.

Due to the continuity of flow in the porous region, the velocity components in the porous region given in (2.4) and (2.5) satisfy the continuity equation (2.1). This results in a Laplace equation in polar form for the squeeze film pressure in the porous region given by

$$\frac{1}{r}\frac{\partial}{\partial r}\left(r\frac{\partial p^*}{\partial r}\right)+\frac{\partial^2 p^*}{\partial z^2}=0 \qquad (2.6)$$

.

The boundary conditions for the velocity components are the no-slip conditions on $z = 0$ and slip condition on $z = h(t)$ given by

$$\begin{aligned} &u=0\,, \quad w=0 \quad \text{on} \quad z=0 \\ &u=0\,, \quad w=w^*+\frac{dh}{dt} \quad \text{on} \quad z=h(t) \end{aligned} \qquad (2.7)$$

and the no-couple stress conditions given by

$$\frac{\partial^2 u}{\partial z^2}=0 \quad \text{on} \quad z=0 \quad \text{and} \quad \text{on} \quad z=h(t) \qquad (2.8)$$

.

The boundary conditions for the squeeze film pressure are

$$p(r_a)=0 \quad \text{and} \qquad (2.9)$$

$$\frac{\partial p}{\partial r}=0 \quad \text{at} \quad r=0 \qquad (2.10)$$

.

The film pressure p^* in the porous matrix satisfies the following conditions

$$p^*(r_a,z)=0 \qquad (2.11)$$

$$\frac{\partial p^*}{\partial z}=0 \quad \text{on} \quad z=h+h^* \qquad (2.12)$$

$$\frac{\partial p^*}{\partial r}=0 \quad \text{at} \quad r=0 \qquad (2.13)$$

where h^* is the thickness of the porous layer. As the film pressure must be continuous at the disk film interface, we have

$$p(r)=p^*(r,h) \quad \text{at} \quad z=h(t)\,. \qquad (2.14)$$

3 Solution Methodology

(2.6) is solved for the film pressure in the porous matrix using the method of separation of variables and using the boundary conditions for film pressure in the porous matrix given in (2.11)-(2.13). The expression for the film pressure in the porous matrix is given by

$$p^* = \sum_{n=1}^{N} c_n e^{\alpha_n z}\left(1 + e^{2\alpha_n\left(h+h^*-z\right)}\right) J_0\left(\alpha_n r\right) \tag{3.1}$$

where $J_0(\alpha_n r)$ is the zeroth order Bessel function and α_n is the n^{th} eigenvalue that satisfies

$$J_0\left(\alpha_n r_a\right) = 0\,. \tag{3.2}$$

The axial momentum equation (2.3) reveals that the pressure p in the film region is independent of z. Then the radial momentum equation (2.2) is solved using the boundary conditions for u given in (2.7) and (2.8). This yields the expression for the radial velocity component u as

$$u = \frac{1}{2\mu}\frac{dp}{dr}\left\{z^2 - hz + 2l^2 - 2l^2\,\frac{\cosh[(2z-h)/2l]}{\cosh(h/2l)}\right\} \tag{3.3}$$

where $l = (\eta/\mu)^{1/2}$ is the couple stress parameter. Substituting the expression of u from (3.3) into the continuity equation (2.1) and integrating across the film thickness we get

$$w\big|_{z=h(t)} - w\big|_{z=0} = \frac{f_0(h,l)}{12\mu}\frac{1}{r}\frac{d}{dr}\left[r\frac{dp}{dr}\right] \tag{3.4}$$

where $f_0(h,l) = h^3 - 12l^2h + 24l^3\tanh(h/2l)$.

Substituting the boundary conditions for the axial velocity component from (2.7) into (3.4), we obtain

$$\frac{f_0(h,l)}{12\mu}\frac{1}{r}\frac{d}{dr}\left[r\frac{dp}{dr}\right] = \frac{dh}{dt} + w^*\,. \tag{3.5}$$

Using the expression for w^* from (2.5), the modified Reynolds equation is derived as

$$\frac{1}{r}\frac{d}{dr}\left[r\frac{dp}{dr}\right] = \frac{12\mu}{f_0(h,l)}\left(\frac{dh}{dt} - \frac{\kappa}{\mu(1-\beta)}\left[\frac{\partial p^*}{\partial z}\right]_h\right). \tag{3.6}$$

From (3.1), we get

$$\left.\frac{\partial p^*}{\partial z}\right|_{z=h} = \sum_{n=1}^{N} c_n\alpha_n e^{\alpha_n h}\left(1 + e^{2\alpha_n h^*}\right) J_0\left(\alpha_n r\right). \tag{3.7}$$

On using the expression for $\partial p^*/\partial z\big|_{z=h}$ from (3.7), the modified Reynolds

equation (3.6) yields

$$\frac{1}{r}\frac{d}{dr}\left[r\frac{dp}{dr}\right]=\frac{12\mu}{f_0(h,l)}\left[\frac{dh}{dt}-\frac{\kappa}{\mu(1-\beta)}\sum_{n=1}^{N}c_n\alpha_n e^{\alpha_n z}\left(1+e^{2\alpha_n h^*}\right)J_0(\alpha_n r)\right] \tag{3.8}$$

Integrating (3.8) twice with respect to r and using boundary conditions (2.9) and (2.12), the squeeze film pressure is obtained as

$$p=\frac{3\mu}{f_0(h,l)}\frac{dh}{dt}\left(r^2-r_a^2\right)+\frac{12\kappa}{f_0(h,l)(1-\beta)}\sum_{n=1}^{N}\frac{c_n e^{\alpha_n h}}{\alpha_n}\left(1-e^{2\alpha_n h^*}\right)J_0(\alpha_n r). \tag{3.9}$$

Substitution of (3.1) and (3.9) in the interface condition (2.14) yields

$$\sum_{n=1}^{N}c_n e^{\alpha_n h}\left[\left(1+e^{2\alpha_n h}\right)-\frac{12\kappa}{f_0(h,l)(1-\beta)}\frac{1}{\alpha_n}\left(1-e^{2\alpha_n h^*}\right)\right]J_0(\alpha_n r)=\frac{3\mu}{f_0(h,l)}\frac{dh}{dt}\left(r^2-r_a^2\right) \tag{3.10}$$

The constants c_n can be determined using the orthogonality of Bessel functions as

$$c_n=\frac{-24\mu}{f_0(h,l)\alpha_n^3}\frac{dh/dt}{r_a J_1(\alpha_n r_a)}\times\left[e^{\alpha_n h}\left\{\left(1+e^{2\alpha_n h^*}\right)-\frac{12\kappa}{f_0(h,l)\alpha_n(1-\beta)}\left(1-e^{2\alpha_n h^*}\right)\right\}\right]^{-1} \tag{3.11}$$

The squeeze film force is found by integrating the squeeze film pressure over the disk surface and is given by

$$f_{sq}=2\pi\int_0^{r_a}pr\,dr \tag{3.12}$$

Introducing the following non-dimensional quantities

$$\begin{aligned}&R=\frac{r}{r_a},\qquad H=\frac{h}{h_0},\qquad H^*=\frac{h^*}{r_a},\quad T=\omega t,\qquad L=\frac{l}{h_0},\\&f_0^*(H,L)=\frac{f_0(h,l)}{h_0^3},\qquad \bar{\alpha}_n=r_a\alpha_n,\qquad \psi=\frac{\kappa h^*}{h_0^3},\qquad P=\frac{h_0^2 p}{\mu\omega r_a^2}\end{aligned} \tag{3.13}$$

where h_0 is the initial film thickness and $1/\omega$ is the characteristic time and substituting (3.11) in (3.9) and applying the non-dimensional quantities given in (3.13), the squeeze film pressure in the non-dimensional form is given by

$$P=\frac{3}{f_0^*(H,L)}\frac{dH}{dT}\left(R^2-1\right)+\sum_{n=1}^{N}\frac{24J_0(\bar{\alpha}_n R)}{f_0^*(H,L)\bar{\alpha}_n^3 J_1(\bar{\alpha}_n)}\frac{dH}{dT}\left\{\frac{f_0^*(H,L)(1-\beta)\bar{\alpha}_n H^*}{12\psi}\frac{\left(1+e^{2\bar{\alpha}_n H^*}\right)}{\left(1-e^{2\bar{\alpha}H^*}\right)}-1\right\}^{-1}. \tag{3.14}$$

The non-dimensional form of the squeeze film force is given by

$$F_{sq}=-\frac{3\pi}{2f_0^*(H,L)}\frac{dH}{dT}+\sum_{n=1}^{N}\frac{48\pi}{f_0^*(H,L)\bar{\alpha}_n^4}\frac{dH}{dT}\left\{\frac{f_0^*(H,L)(1-\beta)\bar{\alpha}_n H^*}{12\psi}\frac{\left(1+e^{2\bar{\alpha}H^*}\right)}{\left(1-e^{2\bar{\alpha}H^*}\right)}-1\right\}^{-1} \tag{3.15}$$

where $F_{sq}=f_{sq}h_0^2/\mu\omega r_a^4$.

The squeeze film pressure and force are obtained for a sinusoidal motion of the upper porous disk $h(t)= h_0+e\sin\omega t$, where h_0 is the initial film thickness, e is the amplitude and ω is the angular frequency of the sinusoidal motion. On using the non-dimensional quantities given in (3.13), the dimensionless form of $h(t)$, with $E = e/h_0$, is given by

(3.16) $$H(T)=1+E\sin T\,.$$

4 Constant Force Squeezing State

Considering constant force squeezing state, the inverse problem is solved and the film thickness and time relation is obtained as

$$\pm 1=\left[-\frac{3\pi}{2f_0^*(H,L)}+\sum_{n=1}^{N}\frac{48\pi}{f_0^*(H,L)\bar{\alpha}_n^4}\left\{\frac{f_0^*(H,L)(1-\beta)\bar{\alpha}_n H^*}{12\psi}\left(\frac{1+e^{2\bar{\alpha}H^*}}{1-e^{2\bar{\alpha}H^*}}\right)-1\right\}^{-1}\right]\frac{dH}{dT} \tag{4.1}$$

where the non-dimensional time is $T=\left|f_{sq}\right|h_0^2 t/\mu r_a^4$. (4.1) is solved numerically for H by fourth order Runge Kutta method using the initial conditions given by

$$H(T=0)=1,\ \frac{dH}{dT}(T=0)=0\,. \tag{4.2}$$

5 Results and Discussion

In this analysis, the effects of couple stresses on the squeeze film behaviour between porous circular disks have been studied on the basis of Stokes microcontinuum theory. The couple stress effects on the squeeze film characteristics is observed through the non-dimensional couple stress parameter L and the effects of permeability through the non-dimensional permeability parameter ψ. The squeeze film pressure and load carrying capacity have been computed using (3.14) and (3.15) for the sinusoidal motion of the upper porous disk.

Figures 2-5 show the variation of non-dimensional squeeze film pressure P as a function of radial co-ordinate R for T=3, β=0.2 and H^*=0.01. Figures 2 and 3 present the squeeze film pressure P with of ψ =0.001 for different values of couple stress parameter L, considering the amplitude of the sinusoidal motion as E=0.2 and E=0.4 respectively. It is observed that the squeeze film pressure P increases for increasing values of couple stress parameter L. Comparing Figures 2 and 3 the squeeze film pressure is more pronounced for larger values of the amplitude of the sinusoidal motion.

Figures 4 and 5 present the variation of non-dimensional squeeze film pressure P as a function of R with L=0.2 for different values of permeability parameter ψ. Figure 4 shows that there is a significant reduction in pressure with increasing permeability of the porous facing for the amplitude of the sinusoidal

motion E=0.2. Also, it has been observed from the graph that there is no significant difference in the pressure distribution between ψ= 0 and ψ= 0.001. Thus ψ= 0.001 indicates a very low permeability almost close to the non-porous case. Similar trend is observed in Figure 5 for E=0.4. Comparing Figures 4 and 5 the squeeze film pressure is more significant for higher values of E although there is a decrease in pressure with increase in permeability.

Figures 6-9 display the variation of non-dimensional squeeze film force F_{sq} as a function of response time T at β=0.2 and H^*=0.01. Figures 6 and 7 present the variation of non-dimensional load carrying capacity F_{sq} with response time T at ψ= 0.001 for different values of couple stress parameter L at E=0.2 and E=0.4 respectively. A significant increase in the load carrying capacity is observed with an increase in the value of couple stress parameter L. i.e. larger the value of couple stress parameter greater is the load carrying capacity. Further, it is observed that the increase in the load carrying capacity is more pronounced for larger values of the amplitude of the sinusoidal motion.

Figures 8 and 9 describe the variation of non-dimensional squeeze film force F_{sq} with response time T for different values of permeability parameter ψ with L=0.2 at E=0.2 and E=0.4 respectively. It has been observed form Figs 8 and 9 the effect of permeability parameter ψ is to decrease the load carrying capacity as compared to the rigid case (ψ= 0) and increase in the load carrying capacity is obtained by increasing the amplitude of the sinusoidal motion. Thus, with a suitable amplitude of the sinusoidal motion, the decrease in the load carrying capacity can be overcome.

The variation of non-dimensional squeeze film thickness H as a function of response time T has been obtained using (4.1) from the constant force squeezing state. Figure 10 presents the gap width as a function of response time for different values of the couple stress parameter L with H^*=0.1, ψ=0.001 and β=0.2. It is observed that, for attaining a particular height there is an increase in the response time with an increase in the couple stress parameter L, i.e. couple stress fluids sustain higher load for a longer time. Figure 11 shows the gap width as a function of response time for various values of the permeability parameter ψ with H^*=0.01, L =0.2 and β=0.2. It is found that the time required for film thickness to reach any particular value is greatly reduced as the permeability parameter increases.

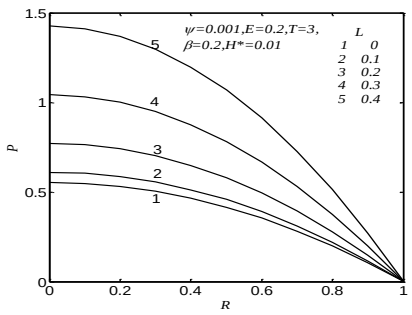

Figure 2 Couple Stress Effects on the Squeeze Film Pressure (E=0.2)

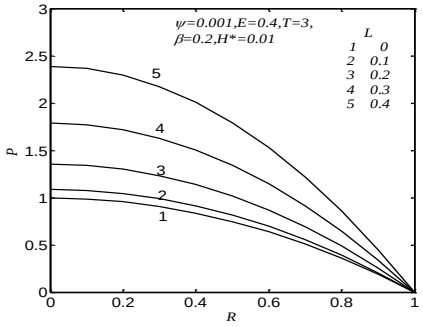

Figure 3 Couple Stress Effects on the Squeeze Film Pressure (E=0.4)

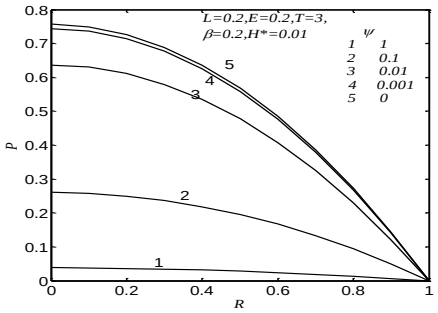

Figure 4 Effects of Permeability on the Squeeze Film Pressure (E=0.2)

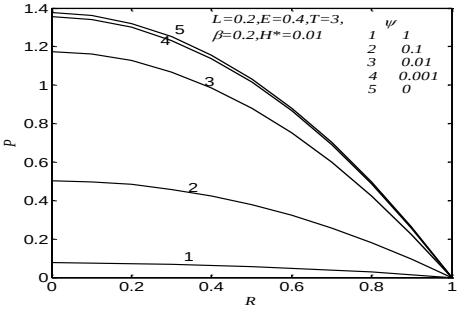

Figure 5 Effects of Permeability on the Squeeze Film Pressure (E=0.4)

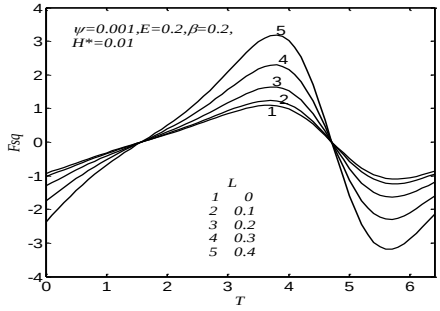

Figure 6 Effects of Couple Stresses on the Squeeze Film Force (E=0.2)

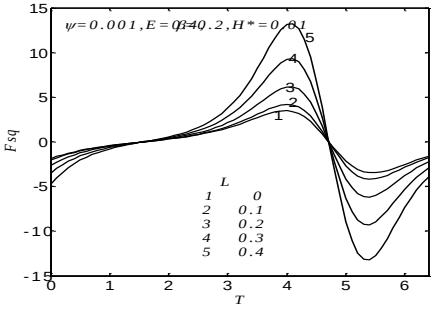

Figure 7 Effects of Couple Stresses on the Squeeze Film Force (E=0.4)

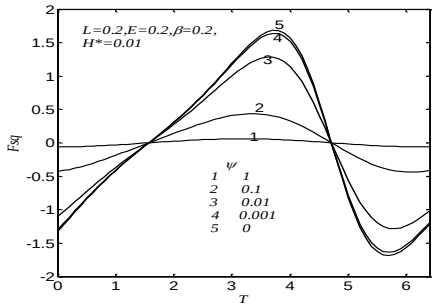

Figure 8 Effects of Permeability on the Squeeze Film Force (E=0.2)

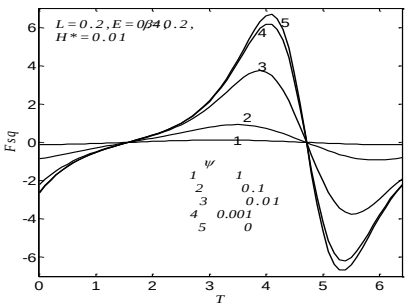

Figure 9 Effects of Permeability on the Squeeze Film Force (E=0.4)

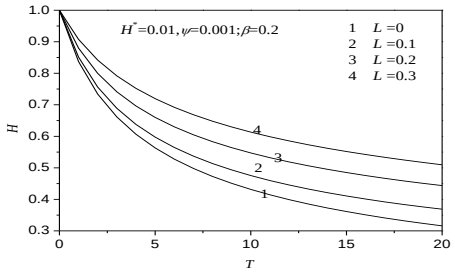

Figure 10 Variation of Couple Stress Parameter on the Film Thickness

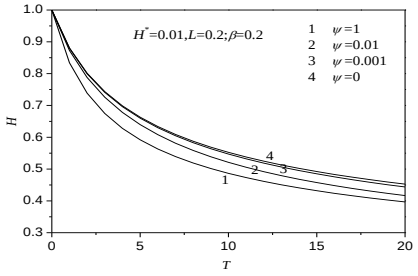

Figure 11 Variation of Permeability Parameter on the Film Thickness

5 Conclusion

The theoretical study of rheological effects of squeeze film flow of a non-Newtonian couple stress fluid between porous circular disks is presented. On the basis of Stokes microcontinuum theory, the modified Reynolds equation is derived and is solved analytically. The numerical results are presented for the sinusoidal motion of the upper disk. An increase in the squeeze film pressure and load carrying capacity is observed for larger values of the couple stress parameter. Further increase of squeeze film pressure and load carrying capacity is obtained by increasing the amplitude of the sinusoidal motion. Although the effect of porous facing on the disk surface decreases the load carrying capacity, the same can be improved by suitably choosing lubricant and amplitude of the sinusoidal motion. Also, it is observed from the inverse problem, the effects of couple stresses provide a longer response time even though the effects of permeability decreases the film thickness. On the whole, the porous squeeze film bearing performance can be improved by the proper choice of lubricants.

References

[1] T. T. Ariman and N. D. Sylvester, Microcontinuum fluid mechanics - A review, *Int. J. Eng. Sci.,* **11** (1973), 905-930.
http://dx.doi.org/10.1016/0020-7225(73)90038-4

[2] T. T. Ariman and N. D. Sylvester, Application of microcontinuum fluid mechanics, *Int. J. Eng. Sci.,* **2** (1974), 273-293.
http://dx.doi.org/10.1016/0020-7225(74)90059-7

[3] N. M. Bujurke and D. P. Basti, Surface roughness effects on squeeze film behaviour in porous circular disks with couple stress fluid, *Trans. Porous Med.,* **71 (**2008), 185-197. http://dx.doi.org/10.1007/s11242-007-9119-2

[4] C. Cusano, Lubrication of porous journal bearings, *ASME Trans. J. Lub. Tech.,* **94** (1972), 69-73. http://dx.doi.org/10.1115/1.3451638

[5] E. A. Hamsa, The magnetohydrodynamic squeeze film, *ASME Trans. J. Tribol.* **110** (1988), 375-377. http://dx.doi.org/10.1115/1.3261636

[6] D. C. Kuzma, Fluid inertia effects in squeeze films, *Appl. Sci. Res.,* **18** (1968), 15-20. http://dx.doi.org/10.1007/bf00382330

[7] P. R. K. Murti, Squeeze film behaviour in porous circular disks, *ASME Trans. J lub Tech.,* **96** (1974), 206-209.

[8] N. B. Naduvinamani and A. Siddangouda, Combined effects of surface roughness and couple stresses on squeeze film lubrication between porous circular stepped plates, *Proc. IMechE partJ:J; Engg Tribol* , Vol. **221**, 2007, 525-534. http://dx.doi.org/10.1243/13506501jet204

[9] N. B. Naduvinamani and A. Siddangouda, Effects of surface roughness on the hydrodynamic lubrication of porous step slider bearings, *Tribol. Int.* **40** (2007), 780-793. http://dx.doi.org/10.1016/j.triboint.2006.07.003

[10] N. B. Naduvinamani, P. S. Hiremath and G. Gurubasavaraj, Squeeze film lubrication of a short porous journal bearing with couple stress fluids, *Tribol. Int.*, **34** (2001), 739-747. http://dx.doi.org/10.1016/s0301-679x(01)00064-0

[11] O. Pinkus and B. Sternlicht, *Theory of Hydrodynamic Lubrication,* Mc-Graw Hill Book Company Inc., New York, 1961.

[12] G. Ramanaiah, Squeeze films between finite plates lubricated by fluids with couple stress, *Wear*, **54** (1979), 315-320. http://dx.doi.org/10.1016/0043-1648(79)90123-6

[13] V. K. Stokes, Couple stress in fluids, *Phys. Fluids.*, **9** (1966), 1709-1715. http://dx.doi.org/10.1063/1.1761925

[14] J. A. Tichy and W. O. Winer, Inertial considerations in parallel circular squeeze film bearings, *ASME Trans. J. Lub. Tech.*, **92** (1970), 588-592. http://dx.doi.org/10.1115/1.3451480

[15] J. A. Tichy, Non-Newtonian lubrication with the convected Maxwell model, *ASME Trans. J. Lub. Tech.*, **118** (1996), 344-348. http://dx.doi.org/10.1115/1.2831307

[16] Vimala Manivasakan and G. Sumathi, Theoretical investigations of couple stress squeeze films in a curved circular geometry, *ASME Trans. J. Tribol.* **133** (2001), 041701-1-8. http://dx.doi.org/10.1115/1.4004099

[17] H. Wu, An analysis of the squeeze film between porous rectangular plates, *ASME Trans. J. Lub. Tech*, **94** (1972), 64-68. http://dx.doi.org/10.1115/1.3451637

Received: December 15, 2014; Published: April 20, 2015